

G-VAE: A CONTINUOUSLY VARIABLE RATE DEEP IMAGE COMPRESSION FRAMEWORK

Ze Cui[†], Jing Wang^{*†}, Bo Bai[†], Tiansheng Guo[†] and Yihui Feng[†]

[†] Huawei, China.

^{*}E-mail: wangjing215@huawei.com

ABSTRACT

Rate adaption of deep image compression in a single model will become one of the decisive factors competing with the classical image compression codecs. However, until now, there is no perfect solution that neither increases the computation nor affects the compression performance. In this paper, we propose a novel image compression framework G-VAE (Gained Variational Autoencoder), which could achieve continuously variable rate in a single model. Unlike the previous solutions that encode progressively or change the internal unit of the network, G-VAE only adds a pair of gain units at the output of encoder and the input of decoder. It is so concise that G-VAE could be applied to almost all the image compression methods and achieve continuously variable rate with negligible additional parameters and computation. We also propose a new deep image compression framework, which outperforms all the published results on Kodak datasets in PSNR and MS-SSIM metrics. Experimental results show that adding a pair of gain units will not affect the performance of the basic models while endowing them with continuously variable rate.

Index Terms— Deep image compression, variational autoencoder, variable rate, gain unit.

1. INTRODUCTION

Image compression is one of the most fundamental and valuable problems in image processing and computer vision to maintain image quality with less storage or transmission. In the last decades, many researchers have worked for the development and optimization of the classical image compression codecs, such as JPEG[28], JPEG2000[26], BPG[3], etc. Based on the inherent redundancy within images, basic modules including transform coding, entropy coding and quantization have been sophisticatedly designed and applied to the classical image compression codecs. Since these modules are artificially designed and optimized separately, it's difficult to adapt to different evaluation indicators and obtain an optimal solution.

Recently, deep learning has achieved significant breakthroughs in various learning problems such as image classification, object detection, etc. Learned image compression framework also has derived significant interests [13, 14, 15, 24, 19, 7, 12, 25, 2, 5, 16, 11, 8, 20]. Thanks to variational autoencoder(VAE) [14, 15, 8, 12, 5, 32], learned image compression methods could achieve much better performance than the classical image compression codecs, e.g. BPG [3], which is an intra-frame encoding of the high efficiency video codec (HEVC) standard [6]. Scalar quantization assumption [14, 15, 19, 7] is proposed to resolve non-differential quantization

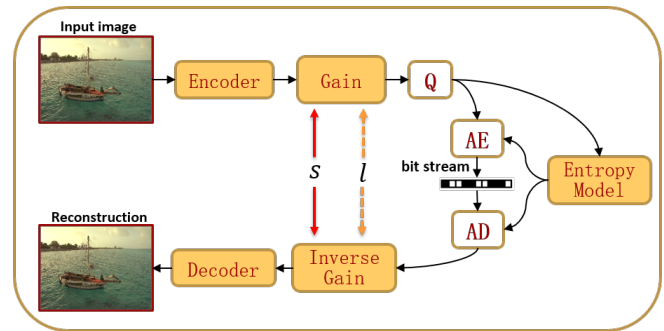


Fig. 1. G-VAE framework. We scale the latent representation channel-wisely by inserting a gain unit after encoder and an inverse-gain unit before decoder, which are jointly optimized with the basic model in the training process. The bit rate could be adjusted flexibly with the pair of gain and inverse-gain vectors, which can be easily calculated from the indexes of the gain vectors s and an interpolation coefficient through $l \in R$.

problem and enable end-to-end training of the VAE framework. In subsequent development of the VAE image compression methods, some researchers introduce a hyperprior network [12] and autoregressive component [5] into the VAE framework to extract accurate prior information of the latent representation, which enhance the entropy estimation. On the other hand, some researchers concentrate on the optimization of the network structure, such as non-local residual block[11], attention mechanism [8, 32] and multiscale fusion [32] to improve feature extraction and reconstruction of the model. With these efforts, the rate-distortion performance of the VAE image compression methods even exceed that of classical image codecs on common metrics, such as Peak Signal-to-Noise Ratio (PSNR) and Multi-Scale-Structural Similarity Index measure (MS-SSIM) [33].

The goal of lossy image compression is commonly to minimize the entropy of the latent representation under a fixed distortion level. The deep image compression methods [14, 15, 8, 12, 5, 32] utilizes the Lagrange multiplier to balance the tradeoff between the bit rate that represents the entropy estimation of quantized latent representation and the distortion that evaluates the error arising from the quantization. In the training process, the Lagrange multiplier is manually set to a fixed rate-distortion tradeoff. Therefore, almost all the deep image compression methods need multiple separate networks trained under different Lagrange multipliers to adapt to different bit rates, in which the training cost and memory requirement increase with the desired rate-distortion points proportionally. Rate adaption of the deep image compression in a single model will become one of

the decisive factors competing with the classical image compression codecs in the future.

In this paper, we propose a novel continuously variable-rate deep image compression framework G-VAE, which introduces a pair of gain units into the VAE framework, as shown in Fig.1. The kernel element of the gain unit is a gain matrix which consists of several gain vectors jointly optimized with the basic network in different Lagrange multipliers. Each pair of gain vectors represents a specific bit rate, and an arbitrary bit rate could be obtained through the interpolation between the pairs of gain vectors. Experiment results show that G-VAE could be introduced into almost all of the VAE-based deep image compression methods and endow them with the characteristic of achieving arbitrary bit rates on the entire rate-distortion curve with negligible additional parameters and computational complexity.

2. RELATED WORKS

Nowadays, lots of learning-based image compression methods [14, 15, 8, 12, 5, 32] adopt variational autoencoders(VAE) as the basic framework. However, almost all of the these methods need to train multiple independent models for different rate-distortion trade-offs. Some researchers have proposed feasible solutions to variable rate image compression methods in a single model by incorporating Recurrent Neural Network (RNN) into the framework [27, 10, 22], adjusting rounding scheme[29, 21] or modifying the inner parts of networks[29, 9].

VAE Framework. The VAE framework could be counted as a non-linear transforming coding model[14, 15]. The transforming process can be mainly divided into four parts: The encoder that maps an image x into a latent representation, $y = f_\theta(x)$; The quantizer that transforms the latent representation into the discrete values, $\hat{y} = Q(y)$; The entropy model that estimates the distribution of \hat{y} to get the minimum rate achievable with lossless entropy source coding [4], $R_\varphi(\hat{y})$; And the decoder that transforms the quantized latent representation to the image, $\hat{x} = g_\phi(\hat{y})$. The entire framework can be trained jointly by optimizing the following loss function

$$\min_{\theta, \phi, \varphi} R_\varphi(Q(f_\theta(x))) + \beta \cdot D(x, g_\phi(Q(f_\theta(x)))) \quad (1)$$

where $R_\varphi(\cdot)$ represents the expected code length (bit rate) of the quantized latent representation and $D(\cdot)$ measures the distortion between the input image and the reconstructed image by a specified evaluation metric. And the Lagrange multiplier β is a constant in the training process to specify rate-distortion performance of the trained model [23]. Therefore, the VAE image compression methods need to use multiple models trained under different β to adjust the different compression performance of images. However, the multi-model scheme only realizes variable rates in several discrete points of rate-distortion curve while memory consumption increases proportionally.

RNN-based Methods. Toderici et al.[27] firstly proposed a novel architecture based on convolutional and deconvolutional Long Short-Term Memory recurrent networks in a progressive style to realize dynamic bit rate, which achieved SOTA results at publication in 2016. In order to improve the performance of the model, the RNN-based scheme successively absorbed better residual scale reconstruction, entropy coding and spatial adaptive bit rates [10, 22] into the framework. However, the rate-distortion performance of the RNN-based scheme is still inferior to JPEG2000[26]. Since bit rate of the RNN-based scheme is proportional to the iterations, variable rates will lead to variable encoding time, making it impractical in applications.

CNN-based Methods. Choi et al. [29] proposed a variable rate image compression framework with a conditional autoencoder, which incorporates fully connection networks into the convolution unit and adjusts compression performance with Lagrange multiplier. In order to extend the coverage from finite discrete points to the whole range of the rate-distortion curve, quantization bin sizes is as the other knob to control quantization loss and finetune bit rate in [29]. However, additional fully connection layers of the conditional convolution increase the computational complexity and memory of the network. Besides, adjustment of quantization bin size influences the rate-distortion performance to some extent and cause dilemma of how to select the best combination of the Lagrange multiplier and quantization size in the intersection of adjacent coarse-adjusting coverages. Yang et al. [9] proposed a modulated autoencoder to realize rate adaption in several discrete points of rate-distortion curve. Similar to conditional autoencoder [29], modulated network introduced fully-connected layers into the autoencoder, which also caused the increase of memory and computation. Akabari et al. [21] proposed stochastic rounding-based quantization scheme and replaced the loss term with rate estimation of the loss function to enable a single model to operate with different bit rates. However, the alteration of loss function makes its performance in PSNR much lower than BPG[3].

Although the above-mentioned methods provide feasible solutions to rate adaption in a single model, they also induce some intolerable problems in practical applications such as performance degradation, computational complexity and memory increase. In this paper, we propose a novel continuously variable rate deep image compression framework G-VAE, which could be applied to almost all the VAE image compression methods and make them achieve continuously variable rate with negligible additional parameters and computation.

3. VARIABLE RATE WITH GAIN UNITS

In the last few years, lots of modules such as hyperprior network[12], attention mechanism[8, 32], etc. have been applied to the VAE image compression framework to achieve better rate-distortion performance. How to endow these VAE image compression methods achieving with variable rate is a great challenge. In this section, we present a new variable-rate image compression framework G-VAE, which can be easily applied to almost all the VAE-based image compression methods without changing the internal structure of the network. The only modification is adding a pair of gain units at the output of encoder and the input of decoder.

3.1. Discrete Variable Rate

The output of the encoder is defined as the latent representation $y \in R^{c \times h \times w}$, where c, h, w represent the number of the channels, the height and the width of the latent representation respectively. Each channel of y can be denoted as $y_{(i)} \in R^{h \times w}$, where $i = 0, 1, \dots, c - 1$. In order to scale the latent representation channel by channel, we develop a gain unit, which is made up of a gain matrix $M \in R^{c \times n}$, where n represents the number of gain vectors. The gain vector can be denoted as $m_s = \{\alpha_{s(0)}, \alpha_{s(1)}, \dots, \alpha_{s(c-1)}\}$, $\alpha_{s(i)} \in R$, where s represents the index of the gain vectors in the gain matrix.

In classical image impression codecs such as JPEG[28], quantization tables have a great influence upon the compression quality as they affect the degrees of compression. These tables are often developed empirically to give the greatest number of bits to the discrete

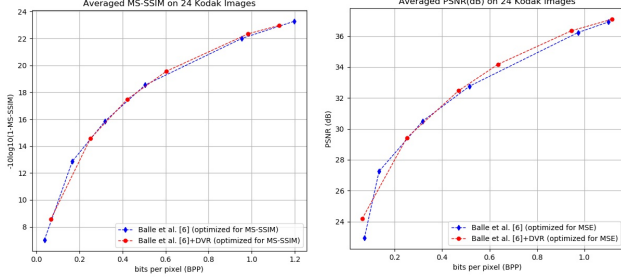


Fig. 2. PSNR and MS-SSIM comparison between our discrete variable rate (DVR) based on G-VAE and the corresponding fixed-rate method [12] on 24 Kodak images. In this experiment, we set n to 6 so that it can produce 6 points of the rate-distortion curve.

cosine transform (DCT) values, which are most noticeable and have the most visible impact. That is, DCT coefficients are treated differently in quantization according to human visual system. Similar to DCT coefficients, different channels of the latent representation also represent different features of the original image. Inspired by the quantization table of JPEG, we could train a gain unit to control the quantization loss according to the channels of the latent representation y , that is

$$\bar{y}_s = G_\psi(y, s) = y \odot m_s \quad (2)$$

where $G_\psi(\cdot)$ represents the gain process, \odot represents channel-wise multiplication, which is $\bar{y}_{s(i)} = y_{(i)} \times \alpha_{s(i)}$, for $i = 0, 1, \dots, c-1$, \bar{y}_s is the gained latent representation, and $\alpha_{s(i)}$ represents the i th gain value in the gain vector m_s . The gain unit can scale the latent representation y to different degrees channelwisely, just like the quantization table, controlling the subsequent quantization error. After that, a quantizer is applied element-wisely to round the gained latent representation \bar{y}_s to the nearest integer

$$\hat{y}_s = Q(\bar{y}_s) = \text{round}(\bar{y}_s) \quad (3)$$

where $Q(\cdot)$ represents the quantization process, \hat{y}_s represents the quantized gained latent representation and $\text{round}(\cdot)$ denotes element-wise rounding to the nearest integer.

Another gain unit is introduced at the input of the decoder to rescale the quantized gained latent representation \hat{y}_s so that the decoder could reconstruct the image correctly. Just like the inverse quantization tables in JPEG [28], we also call it as the inverse gain unit. Consequently, the gain matrix and gain vector in the inverse-gain unit are regarded as inverse-gain matrix $M' \in R^{c \times n}$ and inverse gain vector $m'_s = \{\delta_{s(0)}, \delta_{s(1)}, \dots, \delta_{s(c-1)}\}$, $\delta_{s(i)} \in R$. The inverse-gain process is

$$y'_s = IG_\tau(\hat{y}_s, s) = \hat{y}_s \odot m'_s \quad (4)$$

where $IG_\tau(\cdot)$ represents the inverse gain process, that is $y'_{s(i)} = \hat{y}_{s(i)} \times \delta_{s(i)}$, for $i = 0, 1, \dots, c-1$, and $y'_{s(i)}$ represents the i th channel of the input of decoder, y'_s .

The inverse gain vector m'_s and the corresponding gain vector m_s always appear in pairs, which could be expressed as $\{m_s, m'_s\}$. Each pair of the gain vectors $\{m_s, m'_s\}$ are corresponding to a specific Lagrange multiplier from the predefined finite set of the Lagrange multipliers, $B \in R^n$. The gain vector, inverse-gain vector and Lagrange multiplier are binded together with the subscript s .

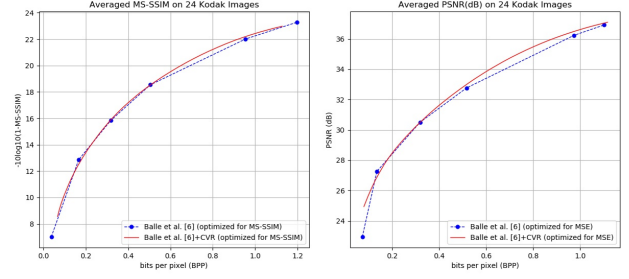


Fig. 3. PSNR and MS-SSIM comparison between our continuously variable rate (CVR) based on G-VAE and the corresponding fixed-rate methods [12] on 24 Kodak images. In this experiment, we set n to 6 and $l \in [0, 1]$ to get a whole range of curve.

Thus, the loss function of G-VAE framework is defined as below

$$\min_{\theta, \phi, \varphi, \psi} \sum_{s=0}^{n-1} R_\varphi(Q(G_\psi(f_\theta(x), s))) + \beta_s \cdot D(x, g_\phi(IG_\tau(Q(G(f_\theta(x), s)), s))) \quad (5)$$

Where $G_\psi(\cdot)$ and $IG_\tau(\cdot)$ represents the gain process and inverse gain process respectively, $R_\varphi(\cdot)$ represents the expected bit rate of the quantized gained latent representation and s represents the index of the gain vectors in the gain matrix.

The effectiveness of G-VAE is firstly validated on the image compression method proposed by Ballé et al. [12]. In the inference process, we change s to obtain the corresponding gain and inverse-gain vector pair, which could be used to adjust the distribution of y and y'_s respectively. By this means, we can obtain the desired compression performance limited to several discrete points of the rate-distortion curve, the distribution of which is decided by the number and value of Lagrange multiplier $\beta_s \in B$. It can be seen from Fig.2 that the rate-distortion performance of our variable rate model in PSNR and MS-SSIM could achieve comparable results with the fixed-rate method.

3.2. Continuous Variable Rate

According to the above description, the gain vectors $\{m_s, m'_s\}$ appear in pairs. In order to ensure that the decoder can generate the image correctly, it is necessary to ensure that the quantized gained latent representation \hat{y} at the input of decoder is at the same scale as the output of encoder. Accordingly, we define

$$m_t \cdot m'_t = m_r \cdot m'_r = C \quad (6)$$

where $\{m_t, m'_t\}$ and $\{m_r, m'_r\}$ ($r, t \in [0, 1, \dots, n-1]$) represent the gain vector pairs corresponding to different bit rates, and $C \in R^c$ is a constant vector. Consequently, a new gain vector pair could be generated by interpolation according to Eq.9. The derivation is as below

$$(m_r \cdot m'_r)^l \cdot (m_t \cdot m'_t)^{1-l} = C \quad (7)$$

$$[(m_r)^l \cdot (m_t)^{1-l}] \cdot [(m'_r)^l \cdot (m'_t)^{1-l}] = C \quad (8)$$

$$m_v = [(m_r)^l \cdot (m_t)^{1-l}], m'_v = [(m'_r)^l \cdot (m'_t)^{1-l}] \quad (9)$$

where $\{m_v, m'_v\}$ is the generated gain vector pair and $l \in R$ is an interpolation coefficient, which controls the corresponding bit rate of

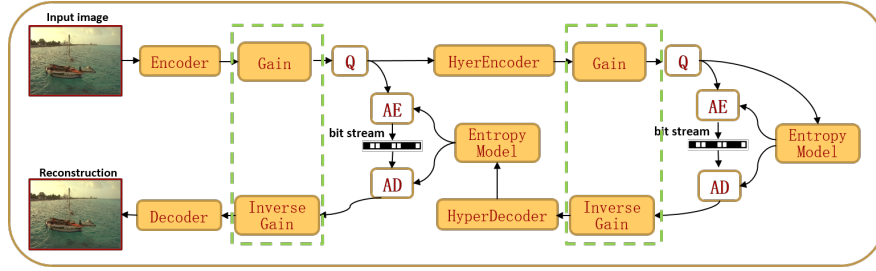


Fig. 4. The extension to hyperprior variable rate image compression method (HCVR).

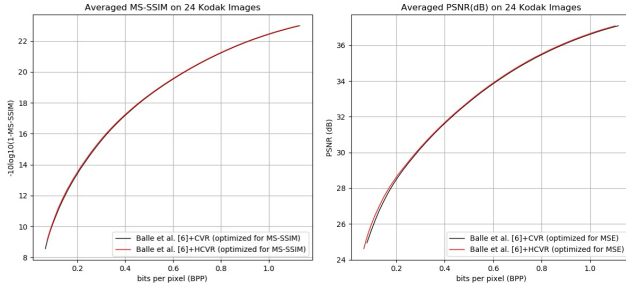


Fig. 5. PSNR and MS-SSIM comparison between HCVR and CVR on 24 Kodak images. The basic model is reproduced from Ballé et al. [12].

the generated gain vector pair. Since l is a real number, an arbitrary bit rate between t and r can be achieved through the interpolation of the gain vector pairs. And when l is equal to 0 or 1, it represents $\{m_t, m'_t\}$ or $\{m_r, m'_r\}$ respectively. It could be proved in Fig.3 that we can extend the coverage from finite discrete points to the whole continuous range of the R-D curve by applying the interpolation between the adjacent gain vector pairs in the inference process.

3.3. Extended To Hyperprior Model

The latent representation can be represented as the Gaussian distribution convolved with a unit uniform noise to ensures a good match between encoder and decoder distributions during training. To capture spatial dependencies in the latent representation and produce a more powerful entropy model for the Gaussian distribution's parameters, the hyperprior network was incorporated into the VAE image compression framework and achieved good rate-distortion performance [12, 5]. In fact, the hyperprior network also adopts an autoencoder structure, which consists of a hyperencoder $f_{\theta_h}(y)$, a hyperdecoder $g_{\phi_h}(z)$ and a quantizer $Q(z)$ (z represents the hyperprior latent presentation). Added to the hyperprior network, the loss function of the framework in Eq.1 is consequently modified as below

$$\min_{\theta, \phi, \psi, \tau, \theta_h, \phi_h, \varphi_h, \psi_h, \tau_h} R_{\varphi}(Q(f_{\theta}(x))) + R_{\varphi_h}(Q(f_{\theta_h}(y))) \quad (10)$$

$$+ \beta \cdot D(x, g_{\phi}(Q(f_{\theta}(x)))) \quad (11)$$

where $R_{\varphi}(\cdot)$ and $R_{\varphi_h}(\cdot)$ represent the entropy estimate model for the latent representation y and hyperprior latent presentation z respectively.

As described in the previous sections, a pair of gain units are inserted after the encoder and before the decoder of the basic framework proposed by Ballé et al. [12] to realize variable rate. Accordingly, another pair of gain unit $G_{\psi_h}(\cdot)$ and inverse gain unit $IG_{\tau_h}(\cdot)$ are introduced into the hyperprior autoencoder to scale the hyperprior z . The entire architecture of the hyperprior continuously

variable rate method (HCVR) based on G-VAE framework is shown in Fig.4. According to the Eq.5 and Eq.10, the loss function of the HCVR method is modified to

$$\min_{\theta, \phi, \psi, \tau, \theta_h, \phi_h, \varphi_h, \psi_h, \tau_h} \sum_{s=0}^{n-1} R_{\varphi}(Q(G_{\psi}(f_{\theta}(x), s))) \quad (12)$$

$$+ R_{\varphi_h}(Q(G_{\psi_h}(f_{\theta_h}(\bar{y}_s), s))) + \beta_s \cdot D(x, g_{\phi}(y'_s)) \quad (13)$$

where \bar{y}_s is the quantized gained latent representation and y' is the inverse gain latent representation. As shown in Fig.5, the performance of extension to HCVR is slightly better than the counterpart of CVR.

4. EXPERIMENTS

In this section, several experiments are designed to verify the effectiveness and efficiency of G-VAE.

4.1. Training

The training set consists of a self-building dataset and a training dataset provided in the Workshop and Challenge on Learned Image Compression (CLIC) [35]. The self-building dataset contains 5000 high-quality images collected in different scenes. These images were downsampled to 2000×2000 pixels and saved as lossless PNGs to avoid compression artifacts. From these downsampled images, we extracted two million patches with size 256×256 to train the network. We incorporated the attention module [30], universal quantization[36, 31], parallel context models [1], hyperprior networks [5] into G-VAE framework, which was called Gained Variational Autoencoder with Attention module and Parallel context model (APG-VAE), to obtain the optimal variable-rate network architecture, which is shown in Fig.6. We trained the model with Adam optimizer [17] for 12 epochs, where the batchsize was set to 8 and the learning rate was initially set to 10^{-4} and reduced to half at the 6th epoch. In our experiments, n denoted the number of gain vector pairs, which was the same as the number of Lagrange multipliers. We prepared two sets of Lagrange multipliers as below

$$B_{m_{ssim}} = \{0.07, 0.03, 0.007, 0.003, 0.001, 0.0006\} \quad (14)$$

$$B_{mse} = \{0.05, 0.03, 0.007, 0.003, 0.001, 0.0003\} \quad (15)$$

where $B_{m_{ssim}}$ and B_{mse} correspond to the models trained with MS-SSIM and MSE loss respectively. In the training process, we randomly select s from 1 to 6 in each iteration to obtain the gain vector m_s , inverse-gain vector m'_s and Lagrange multiplier β_s from gain matrix M , inverse-gain matrix M' and $B_{m_{ssim}/mse}$. The selected gain/inverse-gain vector will be optimized with the corresponding Lagrange multiplier to adapt to different bit rates.

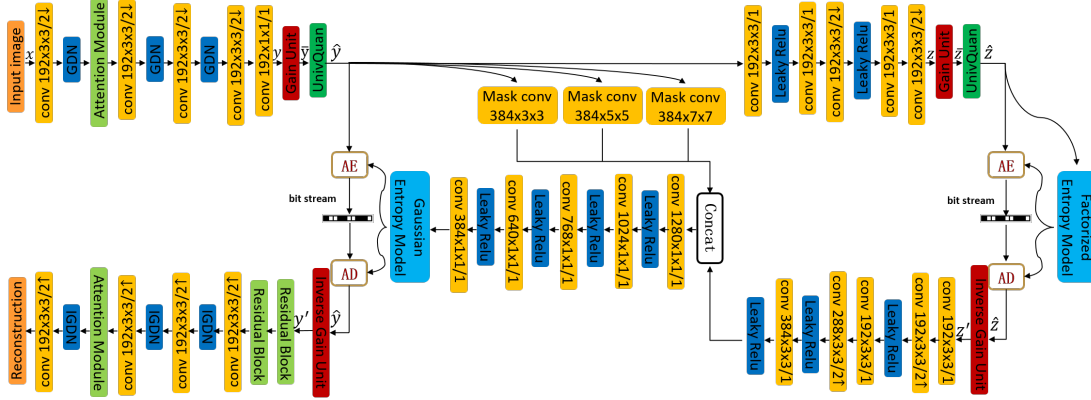


Fig. 6. The architecture of APG-VAE. Convolution parameters are denoted as number of filters \times kernel height \times kernel width / stride, where \uparrow and \downarrow represent upsampling and downsampling respectively. GDN and IGDN represent generalized divisive normalization and the inverse counterpart respectively [13]. Attention Module is used to improve network performance [30]. AE and AD represent arithmetic encoder and decoder. Masked convolution is utilized as [1]. Gain and inverse gain unit have been interpreted above. UnivQuant represents universal quantization [36, 31].

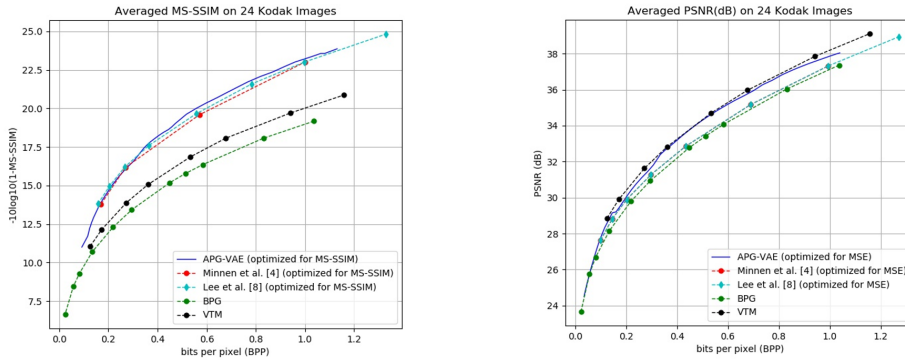


Fig. 7. The comparison between our variable-rate model APG-VAE and the state-of-the-art image compression methods [16, 5, 3, 34] on 24 Kodak images.

4.2. Experimental results

We compared the performance of our variable-rate model APG-VAE to the state-of-the-art learned image compression models from [16, 5] deploying multiple networks trained for varying rates and the classical variable-rate image compression codec BPG [3] on the Kodak image set [18]. Because two different quality metrics are used, the results are presented in two separate plots. As shown in Fig.7, APG-VAE outperforms all the other previous ANN-based methods in both metrics. In particular, the APG-VAE not only outperforms Lee et al. [16] and Minnen et al. [5] which are believed to be the state-of-art ANN-based approach by deploying multiple networks trained for varying bit rates, but also obtains better results than the widely used classical image codec BPG [3] and yields competitive results with VTM [34] in PSNR. Fig.8 shows the variable-rate visual quality comparison of APG-VAE optimized with the MSE loss and BPG [3] on a Kodak image. We adjust the indexes of the gain vectors s and the interpolation coefficient l to adapt and match the compression rate of APG-VAE with the counterpart of BPG [3]. The results show that APG-VAE achieves better visual quality with less artifacts

than BPG [3] at the approximately same BPP.

Since there is no need to modify the internal structure of the network, G-VAE could be easily adapted to almost all the VAE-based image compression methods. We verified the performance of G-VAE on different methods, such as Ballé et al. [12] which has been shown in Fig.3 and Minnen et al. [5] which will be described in the following paragraphs.

According to the process introduced in [5], we reproduced the networks without and with context model, both of which were trained with different Lagrange multipliers separately in order to get multiple fixed-rate models in different bit rates. Then, we added one or two pairs of gain units to these networks, and modified them into the variable-rate models by using the above-mentioned methods, CVR or HCVR. In Fig.9, we compare our variable-rate networks with the corresponding fixed-rate networks in PSNR and MS-SSIM respectively. It could be observed that our variable-rate networks performs very near to the ones individually optimized for several discrete fixed Lagrange multipliers.



Fig. 8. Visual quality comparison of APG-VAE optimized for MSE and BPG [3] on a Kodak image.

4.3. Computational Analysis

Compared with the corresponding fixed-rate models, the additional parameters and computation brought by CVR are described below

$$para_{CVR} = c * n * 2 \quad (16)$$

$$FLOPs_{CVR} = c * h * w * 2 \quad (17)$$

where $para_{CVR}$ and $FLOPs_{CVR}$ represent the additional parameters and computation with gain units of CVR respectively. c, h, w represent the number of channels, height and width of the latent representation respectively and n is the number of the gain vectors used in the gain units of CVR. Besides, the additional parameters and computation amount brought by HCVR are described below

$$para_{HCVR} = c * n * 2 + c_{hp} * n_{hp} * 2 \quad (18)$$

$$FLOPs_{HCVR} = c * h * w * 2 + c_{hp} * h_{hp} * w_{hp} * 2 \quad (19)$$

where $para_{CVR}$ and $FLOPs_{CVR}$ represent the additional parameters and computation with gain units of HCVR respectively, c_{hp}, h_{hp}, w_{hp} represent the number of channels, height and width of the hyperprior latent representation respectively, and n_{hp} is the number of the gain vectors used in the gain units of HCVR. According to the description for the network structures in [12, 5], the parameter percentages P_{para} and P_{FLOPs} computation percentage between additional gain units and original models are computed and shown in the table below.

It can be seen in Table 1 that, compared with the corresponding fixed-rate models, the additional parameters and computation are trivial. Our method can endow the original fixed-rate models

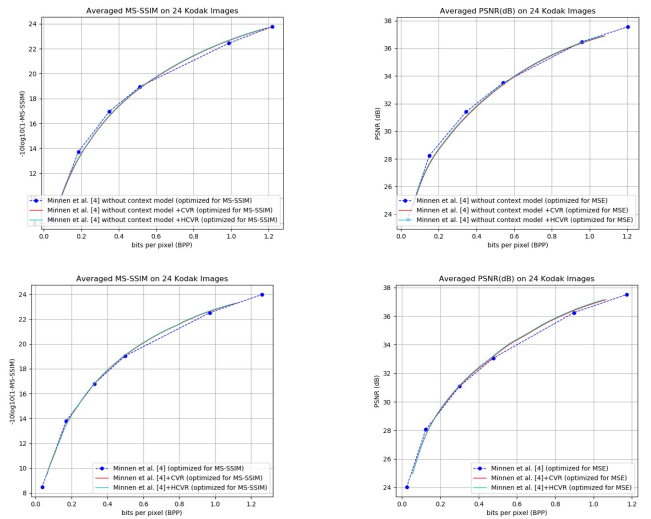


Fig. 9. PSNR and MS-SSIM comparison between CVR, HCVR and the corresponding fixed-rate methods on 24 Kodak images. The basic model in the upper row is to the image compression method without context model proposed by Minnen et al. [5], and the basic model in the bottom row is the image compression method proposed by Minnen et al. [5]. With the same distortion, HCVR could obtain slightly less bit rate than the counterpart of CVR.

Table 1. The percentage of additional parameters and computation ($n = 6, n_{hp} = 6$).

Methods	CVR		HCVR	
	P_{para}	P_{FLOPs}	P_{para}	P_{FLOPs}
Ballé et al. [12]	0.045%	0.00040%	0.076%	0.00042%
Minnen et al. [5]	0.020%	0.00018%	0.040%	0.00019%

with continuous variable-rate characteristics without affecting their performance.

5. CONCLUSION

This paper proposes a novel framework G-VAE, which achieves continuously rate adaption. Unlike the previous solutions, our solution does not need to encode progressively or change the internal unit of the network. The only modification is adding a pair of gain units at the output of encoder and the input of decoder. The solution is so concise that it could be applied to almost all the VAE-based image compression methods and achieve continuously variable rate with negligible additional parameters and computation. We also propose a new deep image compression framework, which outperforms all the published results on Kodak datasets in PSNR and MS-SSIM metrics. Experimental results show that adding a gain units will not affect the performance of the basic model while endowing them with continuously variable rate.

6. REFERENCES

- [1] Aaron Van Den Oord, Nal Kalchbrenner, O.V., Espeholt, L., Graves, A., Kavukcuoglu, K.: Conditional image generation with pixelcnn decoders. *Advances in Neural Information Processing Systems* (2016)
- [2] Ball, J.: Efficient nonlinear transforms for lossy image compression. *Picture Coding Symposium*. pp. 248–252 (2018)
- [3] Bellard, F.: Bpg image format. <https://bellard.org/bpg> (2014)
- [4] Cover, T.M., Thomas, J.A.: *Elements of information theory*. John Wiley and Sons (2012)
- [5] David Minnen, J.B., George, T.: Joint autoregressive and hierarchical priors for learned image compression. *Advances in Neural Information Processing Systems* pp. 10794–10803 (2018)
- [6] Detlev Marpe, H.S., Wiegand, T.: Context-based adaptive binary arithmetic coding in the h.264/avc video compression standard. *IEEE Transactions on Circuits and Systems for Video Technology* **13**(7), 620–636 (2003)
- [7] Eirikur Agustsson, F.M., Tschannen, M., Cavigelli, L., Radu Timofte, L.B., Gool, L.V.: Soft-to-hard vector quantization for end-to-end learning compressible representations. *Advances in Neural Information Processing Systems* (2017)
- [8] Fabian Mentzer, E.A., Tschannen, M., Timofte, R., Gool, L.V.: Conditional probability models for deep image compression. *Proceedings of the IEEE Conference on Computer Vision and Pattern Recognition*. pp. 4394–4402 (2018)
- [9] Fei Yang, L.H., Weijer, J.V.D., Guitian, J.A.I., Lopez, A.M., Mozerov, M.G.: Variable rate deep image compression with modulated autoencoder. *arXiv: Image and Video Processing* (2019)
- [10] George Toderici, S.M.O., Hwang, S.J., Damien Vincent, D.M., Baluja, S., Covell, M., Sukthankar, R.: Full resolution image compression with recurrent neural networks. *Proceedings of the IEEE Conference on Computer Vision and Pattern Recognition* (2017)
- [11] Haojie Liu, T.C., Guo, P., Shen, Q., Cao, X., Wang, Y., Ma, Z.: Non-local attention optimized deep image compression. *Proceedings of the IEEE Conference on Computer Vision and Pattern Recognition* (2019)
- [12] Johannes Ball, D.M., Singh, S., Hwang, S.J., Johnston, N.: Variational image compression with a scale hyperprior. *International Conference on Learning Representations* (2018)
- [13] Johannes Ball, V.L., Simoncelli, E.P.: Density modeling of images using a generalized normalization transformation. *International Conference on Learning Representations* (2016)
- [14] Johannes Ball, V.L., Simoncelli, E.P.: End-to-end optimized image compression. *Picture Coding Symposium* (2016)
- [15] Johannes Ball, V.L., Simoncelli, E.P.: End-to-end optimization of nonlinear transform codes for perceptual quality. *International Conference on Learning Representations* p. 7906310 (2017)
- [16] Jooyoung Lee, S.C., Beack, S.K.: Context-adaptive entropy model for end-to-end optimized image compression. *International Conference on Learning Representations* (2019)
- [17] Kingma, D.P., Ba, J.: Adam: A method for stochastic optimization. *International Conference on Learning Representations* (2015)
- [18] Kodak, E.: Kodak lossless true color image suite (photocd pcd0992) (1993), <http://r0k.us/graphics/kodak>
- [19] Lucas Theis, Wenzhe Shi, A.C., Huszr, F.: Lossy image compression with compressive autoencoders. *International Conference on Learning Representations* (2017)
- [20] Michael Tschannen, Eirikur Agustsson, M., Lucic: Deep generative models for distribution-preserving lossy compression. *Advances in Neural Information Processing Systems*. pp. 5929–5940 (2018)
- [21] Mohammad Akbari, Jie Liang, J.H., Tu, C.: Learned variable-rate image compression with residual divisive normalization. *arXiv: Image and Video Processing* (2019)
- [22] Nick Johnston, Damien Vincent, D.M.e.a.: Improved lossy image compression with priming and spatially adaptive bit rates for recurrent network. *Proceedings of the IEEE Conference on Computer Vision and Pattern Recognition* (2018)
- [23] Ortega, A., Ramchandran, K.: Rate-distortion methods for image and video compression. *IEEE Signal Processing Magazine* **15**(6), 23–50 (1998)
- [24] Rippel, O., Bourdev, L.: Real-time adaptive image compression. *Proceedings of the 34th International Conference on Machine Learning* (2017)

- [25] Shaham, T.R., Michaeli, T.: Deformation aware image compression. *Proceedings of the IEEE Conference on Computer Vision and Pattern Recognition*. pp. 2453–2462 (2018)
- [26] Taubman, D., Marcellin, M.W.: Jpeg2000 image compression fundamentals, standards and practice. *Journal of Electronic Imaging* **11**(2), 286–287 (2013)
- [27] Toderici G, O’Malley S M, H.S.J.e.a.: Variable rate image compression with recurrent neural networks. *International Conference on Learning Representations* (2016)
- [28] Wallace, G.K.: The jpeg still picture compression standard. *IEEE Transactions on Consumer Electronics* **38**(1) (1992)
- [29] Yoojin Choi, M.E., Lee, J.: Variable rate deep image compression with a conditional autoencoder. *Proceedings of the IEEE International Conference on Computer Vision*. (2019)
- [30] Yulun Zhang, K.L., Li, K., Zhong, B., Fu, Y.: Residual nonlocal attention networks for image restoration. *International Conference on Learning Representations* (2019)
- [31] Zamir, R., Feder, M.: On universal quantization by randomized uniform/lattice quantizers. *IEEE Transactions on Information Theory* **38**(2), 428–436 (1992)
- [32] Zhou L, Sun Z, W.X.e.a.: End-to-end optimized image compression with attention mechanism. *Proceedings of the IEEE Conference on Computer Vision and Pattern Recognition Workshops* (2019)
- [33] Zhou Wang, E.P.S., Bovik, A.C.: Multiscale structural similarity for image quality assessment. *Asilomar Conference on Signals, Systems Computers*. **2**, 1398–1402 (2003)
- [34] Versatile video coding reference software version 7.1 (vtm-7.1) (2019), https://vcgit.hhi.fraunhofer.de/jvet/VVCSsoftware_VTM/tags/VTM-7.1.
- [35] Workshop and challenge on learned image compression (2019), <https://www.compression.cc/>
- [36] Ziv, J.: On universal quantization. *IEEE Transactions on Information Theory* **31**(3), 344–347 (1985)